



Taibah University
Journal of Taibah University Medical Sciences

www.sciencedirect.com



Original Article

Morphometric analysis of the main brain sulci and clinical implications:
Radiological and cadaveric study



Sonal Nayak, Msc^a, Chandni Gupta, MD^{a,*}, Karthikeya D. Hebbar, MS^b and
Arvind K. Pandey, PhD^a

^a Department of Anatomy, Kasturba Medical College, Manipal, Manipal Academy of Higher Education, Manipal, India

^b Department of Radiodiagnosis, Kasturba Medical College, Manipal, Manipal Academy of Higher Education, Manipal, India

Received 25 July 2022; revised 8 December 2022; accepted 4 January 2023; Available online 17 January 2023

المخلص

أهداف البحث: يمكن التعرف بسهولة على التلم و تلافيف من المخ بمساعدة الأشعة، ولكن من الصعب تحديد موقعها أثناء العمليات الجراحية بسبب الاختلافات التشريحية والنهج الجراحي للتلم من خلال فتحة صغيرة. لذلك، تم إجراء هذه الدراسة لتحديد موقع التلم الرئيسي للدماغ باستخدام العديد من المعالم التشريحية في عينات الدماغ الجثة وصور الأشعة المقطعية.

طريقة البحث: تمت دراسة 31 عينة دماغ جثة (17 يمينا و 14 يسارا) من جنس (ذكر أو انثى) غير معروف. تمت دراسة 21 معلمة تتعلق بتلمع الدماغ المهم. كما تمت دراسة صور الأشعة المقطعية لما مجموعه 150 مريضا تحت ثلاث فئات عمرية. تم تصنيف معرف المريض على أنه 50 عاما تحت كل فئة عمرية أي 20-40 عاما و 41-60 عاما و 61-80 عاما. تم دراسة 10 معلمات.

النتائج: في عينة الدماغ الجثة على المقارنة اليمنى واليسرى أظهر الجزء الخلفي فقط من التلم الكلسي فرقا كبيرا. في التصوير المقطعي المحوسب ضمن الفئة العمرية، تمت مقارنة الجانب الأيمن والأيسر في كل من الذكور والإناث مما يدل على قيم معنوية للعديد من المعلمات على سبيل المثال التلم الكلسي إلى القطب القذالي الأيمن والأيسر. كما أظهرت المقارنة بين الذكور والإناث نتائج ذات دلالة.

الاستنتاجات: ستساعد هذه الدراسة في تحديد أو إجراء عملية جراحية من قبل جراحي الأعصاب في المناطق الوظيفية المهمة في الدماغ والتي تقع بالقرب من التلم حيث أن التلم متصل بوظائف الجهاز الجيري ويعمل كحاجز للتلافيف.

الكلمات المفتاحية: الأشعة المقطعية؛ التلم المركزي؛ التلم الكلسي؛ التلم الجانبي؛ جراحو الأعصاب

Abstract

Objective: Sulci and gyri of the cerebrum can be easily identified with the aid of radiology but are difficult to locate during surgical operations, owing to anatomical variations and the surgical approach of the sulci through a small aperture. Therefore, this study was performed to locate the main sulci of the brain by using various anatomical landmarks in cadaveric brain specimens and CT scan images.

Methods: In 31 cadaveric brain specimens (17 right and 14 left hemispheres) from people of unknown sex, 21 parameters associated with important sulci of the brain were studied. CT scan images for 150 patients in three age groups were examined. The patient IDs were categorized into 50 patients in each of the following age groups: 20–40 yr, 41–60 yr and 61–80 yr. Ten parameters were studied. The data were statistically analyzed in SPSS software.

Results: In the cadaveric brain specimens, comparisons of right and left hemispheres indicated that only the posterior part of the calcarine sulcus showed a significant difference ($p = 0.0394$). In CT scans within each age group, comparison of the right and left sides in males and females showed significant differences for many parameters (e.g., calcarine sulcus to occipital pole: right $p = 0.0025$; left $p = 0.0009$). Comparisons between male and female parameters also showed significant differences.

* Corresponding address: Department of Anatomy, KMC Manipal, 576104, India.

E-mail: chandnipalimar@gmail.com (C. Gupta)

Peer review under responsibility of Taibah University.



Production and hosting by Elsevier

Conclusion: This study aids in identifying the important functional areas of the brain situated near the sulci, given that the sulci are connected to the gyral functions and act as a barrier for the gyri. The findings may facilitate neurosurgery operations.

Keywords: Calcarine sulcus; Central sulcus; CT scan; Lateral sulcus; Neurosurgeons

© 2023 The Authors.

Production and hosting by Elsevier Ltd on behalf of Taibah University. This is an open access article under the CC BY-NC-ND license (<http://creativecommons.org/licenses/by-nc-nd/4.0/>).

Introduction

Cerebral sulci are the furrows or depressions that demarcate the highly convoluted external surfaces of the brain hemispheres into a series of folds called gyri. These sulci are the extension of the subarachnoid space. They are referred to as fissures when they are deep and anatomically consistent. The primary sulci are 1–3 cm deep, and their walls include tiny interlinked gyri (transverse gyri). The frontal, parietal, occipital, temporal, insular and limbic lobes are categorized according to the primary cerebral sulci and gyri. Superomedial, inferolateral, medial orbital and medial occipital borders divide the superolateral, medial and inferior (basal) surfaces of each cerebral hemisphere. The sulci on the hemisphere's superolateral and inferior surfaces are typically pointed in the direction of the closest ventricular cavity.¹ Therefore, they are also known as the primary microanatomical borders in neurosurgery, because they serve as a point of entry and a path through which surgery can reach the ventricles or deeper lesions.²

The central, callosal, calcarine, parieto-occipital and collateral sulci, and commonly the lateral fissure, are typically continuous.¹ The most consistent (main) sulci are easily distinguished in all normal individuals and show clear relationships with the major functional areas.³

The deepest sulci regions develop early and maintain their individuality. Later, more intricate (and variable) surface folds develop. Quantitative analyses of individual diversity has revealed that deeper brain tissues show relatively low variety and high uniformity among various sulci types. Compared with superficial sulci, deeper sulci show less individual variation.³

The frontal and parietal lobes are separated by the central sulcus (CS). It demarcates or separates the principal motor and somatosensory regions of the cortex, which are located in the precentral and postcentral gyri, respectively. The CS begins in or near the superomedial border (SMB) of the hemisphere, slightly behind the midpoint between the frontal pole (FP) and occipital pole (OP), runs sinuously downward and forward, and typically ends just above the posterior ramus of the lateral sulcus (LS). In both hemispheres, the CS is often continuous, resembling a lengthened letter S.¹

On the superolateral surface of the cerebrum, the LS is the most prominent identifying feature. The sulcus and the sylvian cistern present beneath it form the most commonly used

microneurosurgical corridor, because many cerebral lesions can be reached through this point of entry.² The convergence of the anterior, ascending and posterior branches (rami) of the LS is known as the anterior sylvian (AS) point.² The AS point is surgically important because of the presence of temporal and frontal veins 10–15 mm in front of the AS point and branches of the medial cerebral artery in its deeper region.^{4,5}

The occipital lobe, an essential part of the central nervous system, controls vision. Examinations of this lobe typically focus on its sensory capabilities and the incorporation of the visual pathway.⁶ Its medial surface is traversed by the calcarine sulcus (CalS) and parieto-occipital sulcus (POS). The striate cortex (region 17), which is located in deep regions and the vicinity (surrounding) of the CalS, extends briefly to the lunate sulcus (LunS) on the lateral side of the cerebrum (approximately 1 cm). A “Y” shaped pattern enables easy identification of the CalS and POS. The stem of the “Y” indicates the anterior part of CalS, and the two arms indicate the posterior part of the CalS and POS.⁷ The lateral ventricle shows an elevation called the calcar avis in its posterior horn, which relates to the deeply folded cortical region of the anterior section of the CalS.⁸ The POS originates at the medial surface from the CalS, extends to the SMB, runs up and back, and finally terminates on the superolateral surface. The CalS occasionally meets the LunS, which is not always present and is often oriented vertically.⁹ Magnetic resonance imaging (MRI) allows for the identification of these sulci, thus aiding in mapping of the various striate regions in the occipital lobe. However, these sulci show substantial variations.⁶

Sulci and gyri of the cerebrum can be easily identified with MRI but are difficult to locate during surgical operations because of anatomical variations; the surgical approach of the sulci through a tiny opening; and the presence of nearby structures, such as the arachnoid mater, cerebrospinal fluid and arteries.²

The two most prominent sulci on the superolateral surface of the cerebrum are the CS and LS. The parietal lobe is separated from the occipital by the POS, and the CalS is present in the occipital lobe and is easily observable on the medial surface. A considerable number of studies have examined the cerebral sulci, measuring their length, depth and shape, to aid in approaching the deeper structures.^{2–4,6,9} To our knowledge, many cadaveric brain specimen studies and MRI studies have been conducted on various cerebral sulci. However, no such studies have used CT. Therefore, the current study was aimed at measuring the main sulci of the brain by using various parameters in cadaveric specimens and CT scans, to help anatomists, radiologists and surgeons better localize the sulci and its neighboring functional areas. Understanding of the measurements of these sulci should help radiologists and surgeons approach deeper structures, such as ventricles and subcortical lesions, and perform surgery on the important functional areas located near the sulci.

Materials and Methods

In the current study, cadaveric adult brain hemispheres on both sides (right and left) were examined. The sample size was 31, which consisted of 17 right and 14 left cerebral hemispheres in cadavers of unknown sex. These specimens

were preserved in 10% formalin solution. The age group of these specimens was 60–80 yr, and no pathological disorders were present. Before the study was started, institutional ethical clearance was obtained (IEC: 760/2021). A total of 21 parameters for the measurement of the sulci and its neighboring areas were assessed. The equipment used for the measurements included Vernier calipers, thread, a scale and beaded pins (used to mark reference points). Meningeal coverings were not present, except the firmly adherent pia mater; blood vessels required removal to visualize the sulci clearly. Care was taken not to harm the tissue.

The anatomy of the four main sulci of the cerebrum—the CS, LS, CalS and POS—was studied; these sulci were identified in the specimens.

The parameters measured in the cadaveric brain specimens were as follows (Figures 1 and 2):

- Length of the CS, measured from the beginning point, by marking on the medial surface (upper part) to the termination point of the sulci appearing on the superolateral surface, several millimeters above the LS

On the medial surface:

- Distance of the CS from the FP
- Distance of the CS from the OP
- Distance of the CS from the midpoint of the line joining the FP and OP, taken on the medial surface
- Length of the anterior part (A) of the CalS
- Length of the posterior part (P) of the CalS
- Length of the POS from the bifurcation point to the SMB
- Distance from the posterior end of the splenium to the termination of the CalS in the OP
- Splenium to calcarine-parieto-occipital bifurcation
- Splenium to parieto-occipital end
- POS end to CalS end
- LS–stem length

On the superolateral surface:

- Distance of LS from the inferior margin of the inferior temporal gyrus (ITG)
- Distance of the LS from the superior temporal gyrus (STG)
- Distance from the superior Rolandic (SR) point to the inferior Rolandic (IR) point
- Distance of the AS point from the FP
- Distance of the AS point from the OP
- AS point to the termination of the anterior ramus
- AS point to the termination of the posterior ramus
- AS point to the termination of the ascending ramus
- Distance of the terminal point of the LS from the OP

In addition, the CT scan images of 150 patients who presented to the hospital with mild headache and related symptoms were assessed, according to three age groups. The sample size was calculated with an effect size of 0.6, power of 80%, error of 0.05 and 5% significance with the formula: $n = z^2 \times \sigma^2/d^2$,

where

n = sample needed

z = value of normal standard distribution

σ = standard deviation

d = absolute precision

The patient IDs were collected from the medical records department, and no patients were found to have brain abnormalities or disorders. The patient IDs were categorized into 50 patients in each of the following age groups: 20–40 yr, 41–60 yr and 61–80 yr. Each patient's medical record was opened, and CT scan images of the brain were selected in InstaRad viewer 2.0. The axial plane was used to locate the CS, and the sagittal plane was used for the measurement of parameters in the CT scan images of every patient. The sagittal plane images comprised 5 mm brain slices from side to side; 5 mm slices before the mid-sagittal line were on the right hemisphere, and 5 mm slices immediately after the mid-sagittal line were on the left hemisphere. In the corresponding slices, measurements of possible parameters in centimeters were collected from the right and left sides with a ruler.

The measurements taken from CT scan images included (Figures 3 and 4):

- Distance of the CS from the FP
- Distance of the CS from the OP
- Distance of the CS from the midpoint of the line joining the FP and OP, taken on the medial surface
- Length of the anterior part (A) of the CalS
- Length of the posterior part (P) of the CalS
- Length of the POS from the bifurcation point to the SMB
- Distance from the posterior end of the splenium to the termination of the CalS in the OP
- Splenium to calcarine-parieto-occipital bifurcation
- Splenium to parieto-occipital end
- POS end to CalS end

Because the 5 mm slice near the mid-sagittal line almost showed the medial surface of each hemisphere of the brain, we were able to measure the above described parameters. The remaining parameters could not be measured on the superolateral surface because the surface was uneven.

Statistics

The data were statistically analyzed in Microsoft Excel. Results from morphometric analysis are presented as mean \pm standard deviation (SD). Data were found to be normally distributed; hence, independent t-tests were used to compare the right and left hemispheres in the cadaveric age group (60–80 yr). Independent t-tests were also used to compare the right and left sides of cadaveric specimens, and the CT images of the 60–80 yr age group. The right and left side values for each parameter in males and females were compared within each age group of CT with paired t-tests. CT comparisons among the three age groups were conducted with one way ANOVA. Results with p values less than 0.05 were considered statistically significant. Comparisons between the right and left sides of cadaveric specimens and the CT images in the 60–80 yr age group were performed with independent t-tests.

Results

The sample distribution by sex is shown in Table 1. In the cadaveric brain specimens, the reference points of all

parameters in 31 hemispheres (17 right and 14 left) were relevant and easily identified. The length of the CS and distance from the SR point (the meeting point of the superior extremity of the CS and interhemispheric fissure)

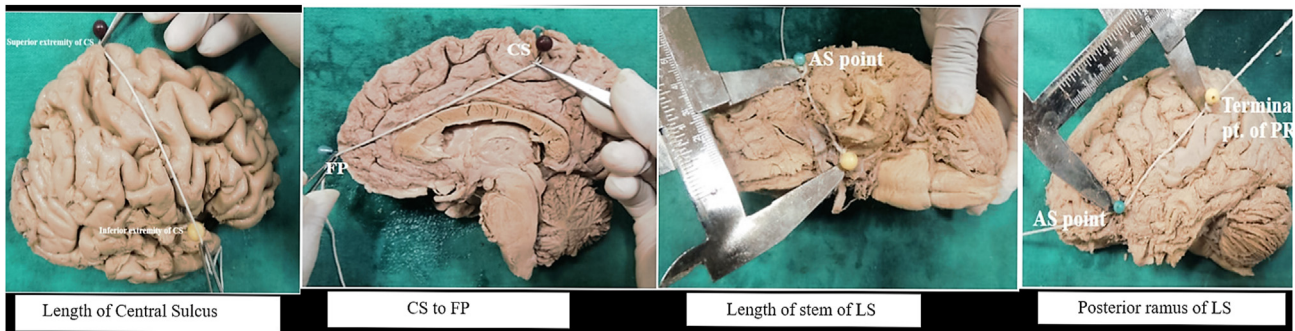


Figure 1: Measurements of the central and lateral sulci in cadaveric brain specimens.

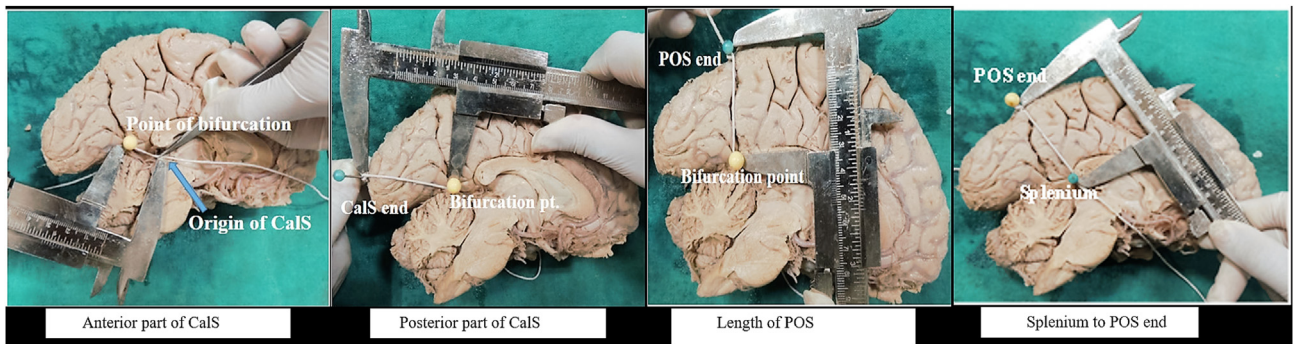
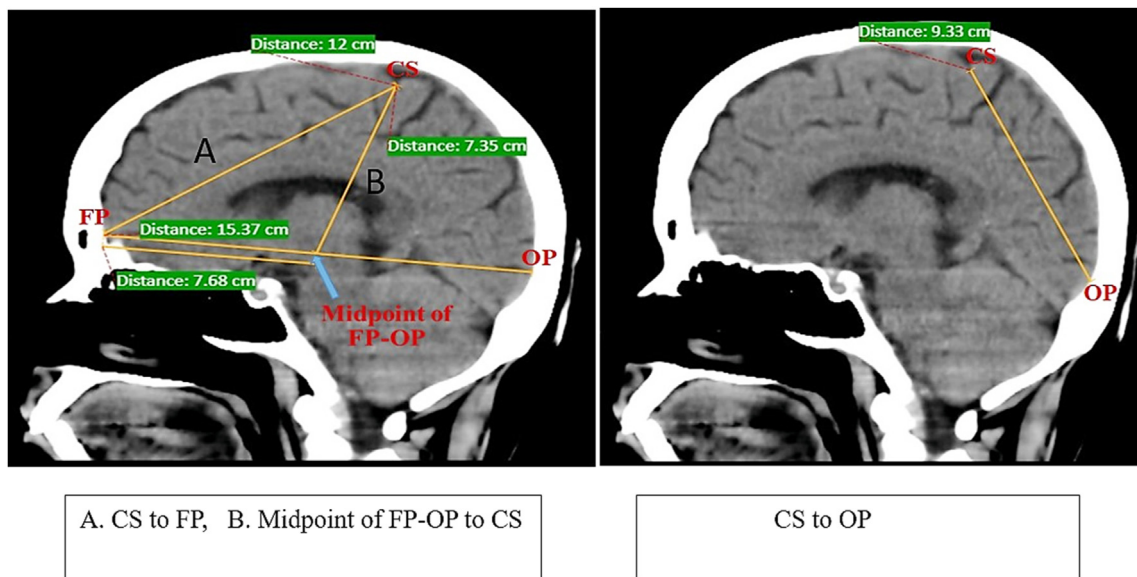


Figure 2: Measurements of the calcarine and parieto-occipital sulci in cadaveric brain specimens.



A. CS to FP, B. Midpoint of FP-OP to CS

CS to OP

Figure 3: Measurements of the central sulcus in CT scans.

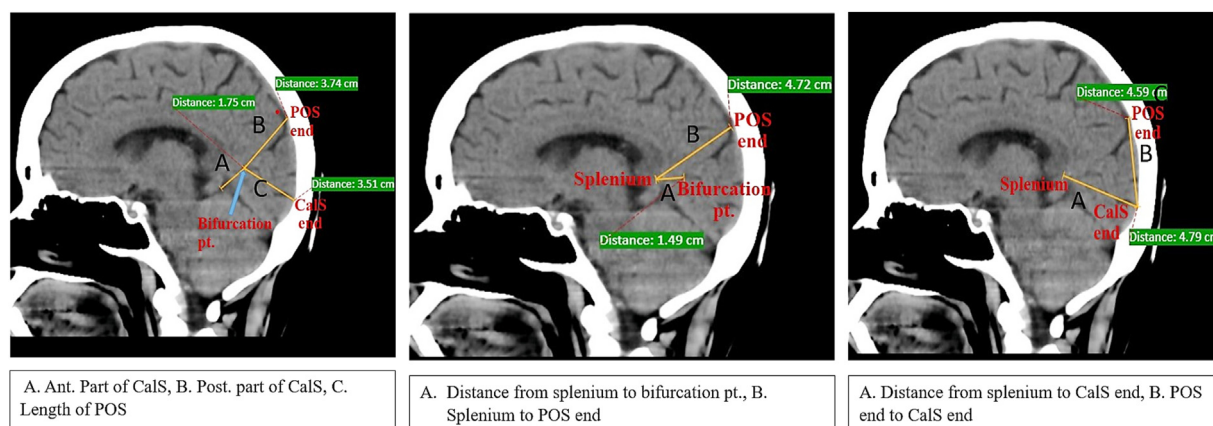


Figure 4: Measurements of the calcarine and parieto-occipital sulci in CT scans.

to the IR point were examined on the superolateral surfaces of all 31 cerebral hemispheres. In all hemispheres, the IR point was clearly above, and did not meet, the LS. In

addition, the CS was found to be continuous. The distance of the CS from the FP, OP, and the midpoint of the line joining the FP and OP was determined on the medial surface. All measurements are shown in [Table 2](#) as mean \pm SD, and no significant differences were observed between the right and left hemispheres.

The AS point was used as a reference to measure the length of the stem, anterior ramus, ascending ramus and posterior ramus of the LS. In addition, the distance from the AS point to the FP and OP was determined. No significant differences were observed between hemispheres. The distances from the terminal point of the LS to the OP, STG and ITG did not significantly differ. Values are indicated in [Table 2](#).

Table 1: Sample distribution by age.

Age	CT scan (n = 150)	
	Male	Female
20–40 (n = 50)	18	32
41–60 (n = 50)	15	35
61–80 (n = 50)	31	19

Table 2: Mean \pm SD of each parameter and independent t-test results comparing right and left side parameters of cadaveric brain hemispheres.

Parameters	Mean \pm SD in cm		p value
	R	L	
CS to FP	11.19 \pm 1.3303	11.61 \pm 0.4185	0.2266
CS to OP	9.06 \pm 0.7611	9 \pm 0.7923	0.8276
Midpoint of the line joining FP and OP to CS	7.49 \pm 0.4854	7.51 \pm 0.6125	0.9211
Anterior part of CalS	2.29 \pm 0.2804	2.19 \pm 0.4305	0.4829
Posterior part of CalS	3.44 \pm 0.4184	3.75 \pm 0.3777	0.0394*
Length of POS (bifurcation point to SMB)	3.34 \pm 0.4152	3.31 \pm 0.5005	0.9012
Posterior end of splenium to CalS end	5.16 \pm 0.3447	5.41 \pm 0.5036	0.1212
Posterior end of splenium to bifurcation point	1.99 \pm 0.3407	1.81 \pm 0.4122	0.2005
Posterior end of splenium to POS end	4.79 \pm 0.3249	4.56 \pm 0.4765	0.1391
POS end to CalS end	4.13 \pm 0.5828	4.03 \pm 0.7363	0.6808
Length of CS	7.16 \pm 0.7826	7.27 \pm 0.7202	0.6863
Length of stem of LS	3.66 \pm 0.5024	3.59 \pm 0.6650	0.7417
Distance of LS from the inferior margin of ITG	3.93 \pm 0.4300	4.02 \pm 0.4023	0.5698
Distance of LS from STG	1.53 \pm 0.5195	1.26 \pm 0.3502	0.0873
Distance from SR to IR point	7.56 \pm 1.2599	7.58 \pm 0.5794	0.9681
Distance of AS point from FP	5.39 \pm 0.5776	5.57 \pm 0.4598	0.3337
Distance of AS point from OP	11.23 \pm 0.6752	11.38 \pm 0.4959	0.4641
AS to termination of AR of LS	1.49 \pm 0.3773	1.48 \pm 0.3613	0.9850
AS to termination of PR	5.49 \pm 0.8291	5.68 \pm 0.5479	0.4506
AS to termination of ascending ramus	1.92 \pm 0.4969	1.89 \pm 0.4047	0.8511
Distance of terminal point of LS from OP	7.46 \pm 0.8397	7.36 \pm 0.7345	0.7218

R: right side, L: left side, CS: central sulcus, FP: frontal pole, OP: occipital pole, POS: parieto: occipital sulcus, SMB: superomedial border, CalS: calcarine sulcus, LS: lateral sulcus, STG: superior temporal gyrus, ITG: inferior temporal gyrus, SR: superior Rolandic point, IR: inferior Rolandic point, AS point: anterior Sylvian point, AR: anterior ramus, PR: posterior ramus of LS.

Table 3: Mean \pm SD of each parameter and one way ANOVA of both right and left sides in males.

Parameters	Age group	Mean (M) \pm SD in cm		p value	
		R	L	R	L
CS to FP	1	11.32 \pm 0.658	11.47 \pm 0.631	0.0861	0.1496
	2	11.39 \pm 0.549	11.49 \pm 0.815		
	3	11.76 \pm 0.845	11.84 \pm 0.739		
CS to OP	1	8.59 \pm 0.693	8.81 \pm 0.679	0.0025*	0.0009*
	2	8.69 \pm 0.455	8.74 \pm 0.459		
	3	9.26 \pm 0.763	9.45 \pm 0.756		
Midpoint of the line joining FP and OP to CS	1	6.14 \pm 0.536	6.27 \pm 0.499	7.64E-07*	4.22E-07*
	2	6.14 \pm 0.292	6.09 \pm 0.557		
	3	7.22 \pm 0.923	7.34 \pm 0.929		
Anterior part of CalS	1	1.61 \pm 0.269	1.58 \pm 0.248	0.0060*	0.0014*
	2	1.9 \pm 0.251	2.02 \pm 0.336		
	3	1.63 \pm 0.297	1.77 \pm 0.359		
Posterior part of CalS	1	3.97 \pm 0.462	3.93 \pm 0.512	0.7811	0.9586
	2	3.93 \pm 0.516	3.98 \pm 0.529		
	3	4.02 \pm 0.378	3.96 \pm 0.407		
Length of POS (bifurcation point to SMB)	1	3.78 \pm 0.375	3.71 \pm 0.552	0.0932	0.1021
	2	4.04 \pm 0.379	3.95 \pm 0.515		
	3	3.78 \pm 0.414	3.61 \pm 0.457		
Posterior end of splenium to CalS end	1	5.43 \pm 0.361	5.20 \pm 0.599	0.0893	0.2433
	2	5.55 \pm 0.479	5.57 \pm 0.479		
	3	5.24 \pm 0.488	5.24 \pm 0.821		
Posterior end of splenium to bifurcation point	1	1.84 \pm 0.419	1.71 \pm 0.394	1.17E-05*	0.8696
	2	1.82 \pm 0.376	1.78 \pm 0.527		
	3	1.31 \pm 0.400	1.66 \pm 0.933		
Posterior end of splenium to POS end	1	5.27 \pm 0.546	5.07 \pm 0.58	0.8918	4.09E-05*
	2	5.42 \pm 0.336	5.19 \pm 0.466		
	3	4.51 \pm 0.505	4.53 \pm 0.434		
POS end to CalS end	1	5.14 \pm 0.635	4.92 \pm 0.587	0.0798	0.2331
	2	5.25 \pm 0.585	5.3 \pm 0.511		
	3	4.81 \pm 0.746	4.92 \pm 0.894		

*p < 0.05 is significant.

Table 4: Mean \pm SD of each parameter and one way ANOVA of both right and left sides in females.

Parameters	Age group	Mean (M) \pm SD in cm		p value	
		R	L	R	L
CS to FP	1	11.02 \pm 0.738	11.01 \pm 0.741	0.1022	0.5609
	2	10.96 \pm 0.701	11.03 \pm 0.809		
	3	11.38 \pm 0.649	11.24 \pm 0.789		
CS to OP	1	8.22 \pm 0.707	8.43 \pm 0.843	0.0102*	0.0024*
	2	8.08 \pm 0.642	8.17 \pm 0.667		
	3	8.71 \pm 0.859	8.93 \pm 0.718		
Midpoint of the line joining FP and OP to CS	1	5.97 \pm 0.695	6.09 \pm 0.729	0.0012*	0.0019*
	2	5.8 \pm 0.609	5.85 \pm 0.560		
	3	6.59 \pm 1.001	6.63 \pm 1.036		
Anterior part of CalS	1	1.55 \pm 0.229	1.54 \pm 0.265	0.0027*	0.0001*
	2	1.78 \pm 0.291	1.88 \pm 0.308		
	3	1.62 \pm 0.285	1.68 \pm 0.358		
Posterior part of CaS	1	3.76 \pm 0.356	3.74 \pm 0.391	0.3588	0.9899
	2	3.68 \pm 0.471	3.75 \pm 0.438		
	3	3.84 \pm 0.349	3.73 \pm 0.366		
Length of POS (bifurcation point to SMB)	1	3.71 \pm 0.428	3.63 \pm 0.384	0.8808	0.3748
	2	3.74 \pm 0.585	3.67 \pm 0.508		
	3	3.67 \pm 0.442	3.50 \pm 0.315		
Posterior end of splenium to CalS end	1	5.19 \pm 0.461	5.15 \pm 0.481	0.2983	0.0199*
	2	5.13 \pm 0.535	5.28 \pm 0.434		
	3	4.97 \pm 0.445	4.88 \pm 0.599		
Posterior end of splenium to bifurcation point	1	1.76 \pm 0.409	1.74 \pm 0.396	9.36E-05*	0.0003*
	2	1.74 \pm 0.381	1.74 \pm 0.368		
	3	1.24 \pm 0.547	1.29 \pm 0.474		
Posterior end of splenium to POS end	1	5.07 \pm 0.394	4.96 \pm 0.455	7.46E-06*	7.59E-05*
	2	4.92 \pm 0.361	4.92 \pm 0.437		
	3	4.45 \pm 0.540	4.30 \pm 0.759		
POS end to CalS end	1	4.89 \pm 0.455	4.94 \pm 0.563	0.0077*	0.0025*
	2	4.82 \pm 0.598	4.81 \pm 0.664		
	3	4.39 \pm 0.639	4.3 \pm 0.687		

*p < 0.05 is significant.

Table 5: Right and left side comparison in males and females of each age group.

Parameters	Age group	p value	
		M	F
CS to FP	1	0.2913	0.9118
	2	0.5156	0.5299
	3	0.3561	0.3779
CS to OP	1	0.1822	0.0453*
	2	0.5405	0.3282
	3	0.0675	0.1512
Midpoint of the line joining FP and OP to CS	1	0.3389	0.1395
	2	0.7215	0.6662
	3	0.1100	0.8045
Anterior part of CalS	1	0.7153	0.8795
	2	0.1754	0.0755
	3	0.0187*	0.5131
Posterior part of CalS	1	0.6264	0.7073
	2	0.6254	0.3656
	3	0.3189	0.2145
Length of POS (bifurcation point to SMB)	1	0.2940	0.3027
	2	0.3372	0.4660
	3	0.0477*	0.1149
Posterior end of splenium to CalS end	1	0.0164*	0.3824
	2	0.7496	0.0512
	3	0.9775	0.2001
Posterior end of splenium to bifurcation point	1	0.1123	0.7224
	2	0.7687	1
	3	0.0451*	0.2697
Posterior end of splenium to POS end	1	0.1072	0.0085*
	2	0.0041*	1
	3	0.7367	0.1257
POS end to CalS end	1	0.1402	0.5189
	2	0.6508	0.9379
	3	0.4508	0.5152

*p < 0.05 is significant.

The lengths of the anterior and posterior parts of the CalS, and of the POS from the bifurcation point to the SMB were measured; no significant differences between hemispheres were observed, except in the posterior part of the CalS ($p = 0.0394$). In two of the right hemispheres, ramification at the distal end of the POS was observed. In most cases (61%), the CalS did not meet the LunS. Distance was measured from the posterior end of the splenium to the termination of the CalS in the OP, calcarine-parieto-occipital

bifurcation and POS end. The distance from the POS end to the CalS end was also noted. No significant differences were found between hemispheres.

In CT, comparisons of male right, male left, female right and female left parameters among the three age groups were conducted with ANOVA (Tables 3 and 4 for males and females, respectively). Among all parameters, the CS to OP, the anterior part of the CalS, the midpoint of the line joining the FP and OP to the CS on both the right and left

Table 6: Comparisons between the right and left sides of cadaveric specimens and CT image parameters of the 60–80 yr age group with independent t-tests.

Parameters	p value	
	Right	Left
CS to FP	0.2224	0.9946
CS to OP	0.9482	0.3009
Midpoint of the line joining FP and OP to CS	0.0069*	0.0495*
Anterior part of CalS	5.04E-09*	0.0019*
Posterior part of CalS	0.0001*	0.2961
Length of POS (bifurcation point to SMB)	0.0017*	0.0946
Posterior end of splenium to CalS end	0.8613	0.0783
Posterior end of splenium to bifurcation point	6.61E-08*	0.0783
Posterior end of splenium to POS end	0.0066*	0.4376
POS end to CalS end	0.0052*	0.0090*

*p < 0.05 is significant.

sides, the posterior end of the splenium to the bifurcation point on the right side, and the posterior end of the splenium to the POS end on the left side in males showed significance with the ($p < 0.05$). In females, the CS to OP, midpoint of the line joining the FP and OP to the CS, the anterior part of the CalS, the POS end to CalS end, the posterior end of the splenium to the bifurcation point, and the posterior end of the splenium to the POS end showed significance on both the right and left sides ($p < 0.05$). The posterior end of the splenium to the CalS end on the left side showed a p value of 0.0199.

Within each age group, the right and left sides were compared in both males and females, and the p values are shown in Table 5. The anterior part of the CalS ($p = 0.0187$), the length of the POS from the point of bifurcation to the SMB ($p = 0.0477$), and the posterior end of the splenium to the bifurcation point ($p = 0.0451$) in males 60–80 yr of age; the posterior end of the splenium to the CalS end ($p = 0.0164$) in males 20–40 yr of age; and the posterior end of the splenium to the POS end ($p = 0.0041$) in males 40–60 yr of age showed significance. In females, the CS to OP ($p = 0.0453$), and the posterior end of the splenium to the POS end ($p = 0.0085$), in the 20–40 yr age group showed significant differences between hemispheres.

Comparisons between the right sides and left sides of cadaveric specimens and the CT images of the 60–80 yr age group were performed with independent t -tests (Table 6). The right side mean value of cadaveric specimens was compared with that of CT in the 60–80 yr age group with independent t -tests. The posterior part of the CalS showed significance, with $p = 0.0001$. The length of the POS (from the bifurcation point to SMB), and the distance from the posterior end of the splenium to the POS end also showed significance, with $p = 0.0017$ and 0.0066, respectively. The posterior end of the splenium to the bifurcation point also showed significance ($p < 0.05$). On both sides, the midpoint of the line joining the FP and OP to the CS, the anterior part of the CalS sulcus, and the POS end to the CalS end were found to show significance ($p < 0.05$).

Discussion

The CS divides the primary motor cortex (pre central gyrus) and the primary sensory cortex (post central gyrus). Voluntary movement is controlled primarily by the area in the frontal lobe just anterior to the CS (area 4). The anterior portion of the parietal lobe is the primary sensory area, which receives sensory information from the body. The LS (Sylvian fissure) demarcates the frontal and the parietal lobe from the temporal lobe. The adjacent areas of this sulcus include Broca's area and Wernicke's area, which are situated in the frontal and temporal lobes, respectively. The POS can be clearly seen on the medial surface, and part of it extends into the superolateral surface. The cuneus and precuneus are separated from each other on the medial surface by this sulcus. The precuneus is involved in functions including episodic memory, visuospatial processing and aspects of consciousness. The cuneus (Brodmann area 17) receives visual information from the same-sided quadrant retina (corresponding to the contralateral inferior visual field). Lesions in the occipital striate cortex (BA 17) produce areas of blindness in the contralateral visual field. The CalS is

associated with the visual association cortex, because it is bounded by the cuneus and lingual gyrus on the medial surface of the occipital lobe.

The LS is associated with Broca's area (left inferior frontal gyrus), which is responsible for speech production and language processing, and Wernicke's area (left posterior STG), which is responsible for speech comprehension. We measured the length of the anterior ramus, ascending ramus and posterior ramus of the LS by using the AS point as a reference. All hemispheres were evaluated for the presence of the AS point, which was found in the expanded region of LS, specifically in the anterior-inferior part of the pars opercularis and below the pars triangularis of the inferior frontal gyrus. Gonul et al. have reported the same location of the AS point and used it as a reference point for measurement of the rami of the LS.² Ribas et al. have reported that the AS was found in the same location in 4.16% of right hemispheres and 6.38% of left hemispheres in 18 cadavers.⁴ Juch et al. have found an absence of the anterior ramus on the right hemisphere in 13% of cases and none on the left hemisphere.¹⁰ In 104 specimens, Tomaiuolo et al. have noted that 1.9% lacked the ascending ramus.¹¹ Ono et al. have reported absent rami on the right side in 16% and on the left side in 8% of cases.¹² Witelson and Kigar have found no correlation between sylvian fissure morphology and hand preference in women; however, in men, functional asymmetries were associated with the anatomy of sylvian fissure.¹³ Gonul et al. have measured the anterior ramus, ascending ramus and posterior ramus lengths of the LS on both right and left cerebral hemispheres and reported values of 23.30 ± 8.120 (mean \pm SD) (Right), 22.66 ± 6.751 (Left), 27.64 ± 5.784 (Right), 27.60 ± 6.731 (Left), 76.00 ± 9.691 (Right) and 77.50 ± 10.54 (Left) mm, which are greater than those obtained in our study i.e., 1.49 ± 0.377 (Right), 1.48 ± 0.361 (Left), 1.92 ± 0.4969 (Right), 1.89 ± 0.4047 (Left), 5.49 ± 0.8291 (Right) and 5.68 ± 0.5479 (Left) cm on the right and left side of the hemisphere, respectively.² In our study, we also included measurement of the length of the stem of the LS, the distance from the AS point to the FP and OP, the distance from the terminal point of the LS to the OP, and the ITG and STG. Boni et al. have reported that the distance from the terminal point of the LS to the inferior margin of the ITG in the right hemisphere is 46.86 mm (medium number), and that in the left hemisphere is 44.28 mm (5.95% higher in the right hemisphere).¹⁴ In our study, the distance from the terminal point of the LS to the inferior margin of the ITG was measured as 3.93 ± 0.4300 (mean \pm SD) and 4.02 ± 0.4023 cm on the right and left sides, respectively.

CS, an important sulcus that is present on the superolateral surface of the cerebrum, and separates the motor and the sensory area, was found to be continuous in all specimens in our study. Gonul et al. have reported continuity of CS in 99% of specimens.² Juch et al., in an MRI investigation in 23 participants, have found CS continuity in 100% of right hemispheres and 91% of left hemispheres.¹⁰ Ono et al. have found that the CS was continuous in 92% of cases, interrupted in 8% of cases or connected to the pre-CS in the inferior region.¹² Most researchers, including Retzius, have reported that only 1% of specimens have CS discontinuity.¹⁵ Our findings are in agreement with those from most studies in the literature. The mean length of CS observed by Jabeen et al. in males and females was

10.51 ± 0.529 cm to 9.78 ± 0.996 cm, and 10.27 ± 0.786 cm to 8.83 ± 0.379 cm, respectively. In addition, the CS depth in males ranged from 1.333 ± 0.100 cm to 1.029 ± 0.125 cm, and that in females ranged from 1.173 ± 0.144 cm to 1.01 ± 0.200 cm.¹⁶ In our study, the depth of the CS was not measured, but the mean length was found to be 7.16 ± 0.7826 cm on the right side and 7.27 ± 0.7202 cm on the left side. Ono et al. have reported mean lengths of the CS of 105 mm on the right hemisphere and 94 mm on the left hemisphere.¹² Singh and Gupta have reported mean lengths of the CS of 94.75 mm and 96.06 mm on the right and left hemispheres, respectively, among 34 hemispheres examined. When the sulcal length of two hemispheres was compared, the p value (0.6242) was found to be insignificant.¹⁷ In our study, the length of CS was greater on the left than the right side, but a comparison between hemispheres indicated an insignificant p value (0.6863). The SR point was noted in all specimens, because it is the point of intersection of the superior extremity of CS and interhemispheric fissure. In an MRI investigation by Juch et al., in 13% of the specimens, the CS and interhemispheric fissure (IHF) were not combined.¹⁰ Most well-known earlier research has indicated that the upper extremity of the CS is present in the IHF in at least 88% of cases. According to Retzius, the CS is present in the IHF in 64% of cases, mixed or adjacently present to the IHF in 16% of cases, and separately present in 20% of cases.¹⁵ In an investigation by Ono et al., the upper extremity of the CS extended toward the IHF in 56/72% (right/left hemispheres).¹² The lower extremity of the CS in our study was found to be several millimeters higher than the LS in all specimens. The lower extremity of the CS has been observed by Gonul et al. to be higher above the LS in 72% of cases, and to be combined or inside the LS in 28% of cases.² Ono et al. have observed that the inferior extremity of the CS meets the LS in 16% of right and 19% of left hemispheres.¹² Ribas et al. have found that the CS inferior extremity meets the LS in 17% of specimens.⁴ We did not observe meeting of the CS and LS in our study, possibly because of the small sample size of specimens. The distance between the SR and the IR points reported by Gonul et al. was 93.58 ± 7.511 mm on the right side and 98.44 ± 7.293 mm on the left side.² Our results showed smaller values of 7.56 ± 1.2599 on the right side and 7.58 ± 0.5794 cm on the left side. We also measured the distance of the CS from the FP, OP and the midpoint of the line joining the FP and OP in both cadaveric and CT samples.

CalS is bounded by the cuneus above and the lingual gyrus below. Area around the CalS is the visual cortex and visual association cortex. In the posterior IHF region, the CalS is the most important anatomical reference. Flores, in an investigation of 26 brain specimens, has found that the CalS develops straight from the parahippocampal gyrus, and the sulcus is not constant at its termination.⁶ Mandal et al. have studied 106 specimens and observed variations near the termination of CalS.⁹ According to Flores, *nf.*⁶ Mandal et al. have found no rami at the sulcus termination in 40.56%, divided once in 55.66%, divided twice in 3.77%, crossed OP in 57.69%, and in 31.13% CalS met the LunS. In addition, variations in the length and shape of the LunS were observed.⁹ Both Flores and Mandal et al. have shown the same percentage of sulci crossing the OP.^{6,9} Our current study indicated that the CalS

arose from the parahippocampal gyrus in all specimens; in 61% of cases, the CalS did not meet the LunS. Ramification of the CalS was not noted. The lengths of the anterior and posterior parts of the CalS were 2.73 ± 9.95 and 4.12 ± 1.44 cm, respectively, in Mandal et al.⁹ In the current study, the anterior part of the CalS was 2.29 ± 0.2804 (R) or 2.19 ± 0.4305 (L), and the posterior part was 3.44 ± 0.4152 (R) or 3.75 ± 0.3777 (L) cm. The posterior part had a longer length than the anterior part, as also described by Mandal et al.⁹

The POS is a deep sulcus that marks the boundary between the cuneus and precuneus on the medial surface. The distance from the posterior end of the splenium to the bifurcation point (2.02 cm), and the bifurcation of CalS to the end of the POS (3.42 cm), were measured by Mandal et al.⁹ Herein, we determined the distance from the posterior end of the splenium to the bifurcation point (1.9 cm), and the bifurcation of the CalS to the end of the POS (4.08 cm).

Knowledge of the locations of these sulci in relation to various anatomical landmarks should facilitate the approach to subcortical lesions and permit safer access to deep structures in surgeries in areas surrounding these sulci.

Limitations

1. The sample size of cadaveric specimens was small.
2. Not all parameters were measured in CT scans because of difficulty in localizing all sulci.

Conclusion

The morphometry of the four main sulci of the cerebral hemisphere was studied in cadaveric brain specimens and CT scans. In the cadaveric specimens, only one parameter was found to significantly differ between sides. In comparison, in CT, many parameters were found to significantly differ, thus indicating asymmetries between the cerebral hemispheres. The underlying structures were closely associated with some of the topographic sites evaluated in this study. Thus, knowledge of the measurements of these sulci may aid radiologists and surgeons in approaching deeper structures, such as ventricles and subcortical lesions.

This study should also facilitate identifying or performing surgery on the important functional areas of the brain situated near the sulci, because the sulci are connected to the gyral functions and act as a barrier for the gyri.

The use of functional CT images herein helped correlate the measurements with those from the cadaveric specimens, and facilitated better localization of the positions of sulci and the functional areas.

We believe that this study meets an important need, because prior studies have examined the cerebral sulcus morphometry in cadaveric brain specimens, and a few MRI studies have been associated with sulci, but no studies have used CT.

Source of funding

This research did not receive any specific grant from funding agencies in the public, commercial, or not-for-profit sectors.

Conflict of interest

The authors have no conflict of interest to declare.

Ethical approval

Ethical clearance was obtained from the institutional ethics committee (date: 10/11/2021), IEC no. 760/2021.

Authors contributions

CG conceived and designed the study, and wrote the final draft of the article. SN conducted research, collected and organized data, analyzed and interpreted data, and wrote the initial draft of the article. KDH provided research, wrote materials and provided logistic support. AKP wrote the final draft of the article. All authors have critically reviewed and approved the final draft and are responsible for the content and similarity index of the manuscript.

Acknowledgments

The authors acknowledge Dr. Prasanna LC, Professor and Head, Department of Anatomy, Kasturba Medical College, Manipal, and Dr. Prakashini, Professor and Head, Department of Radiodiagnosis, Kasturba Medical College, Manipal, for allowing the authors to conduct the study in the department.

References

1. Standring S, editor. *Gray's anatomy e-book: the anatomical basis of clinical practice*. Chapter 25 cerebral hemisphere. Elsevier Health Sciences; 2021. p. 373.
2. Gonul Y, Songur A, Uzun I, Uygur R, Alkoc OA, Caglar V, Kucuker H. Morphometry, asymmetry and variations of cerebral sulci on superolateral surface of cerebrum in autopsy cases. *Surg Radiol Anat* 2014; 36(7): 651–661.
3. Lohmann G, Von Cramon DY, Colchester AC. Deep sulcal landmarks provide an organizing framework for human cortical folding. *Cerebr Cortex* 2008; 18(6): 1415–1420.
4. Ribas GC, Ribas EC, Rodrigues CJ. The anterior sylvian point and the suprasylvian operculum. *Neurosurg Focus* 2005; 18(6): 1–6.
5. Yasargil MG, Krisht AF, Türe U, Al-Mefty O, Yasargil DC. Microsurgery of insular gliomas: part I—surgical anatomy of the sylvian cistern. *Contemp Neurosurg* 2017; 39(11): 1–8.
6. Flores LP. Occipital lobe morphological anatomy: anatomical and surgical aspects. *Arq Neuropsiquiatr* 2002; 60: 566–571.
7. Central nervous system. In: Mc Minn RMH, editor. *Last's anatomy regional and applied*. 9th ed. 151. London: Churchill Livingstone; 1994. pp. 579–591.
8. Crossman AR. Cerebral hemisphere. In: Standring S, editor. *Gray's anatomy the anatomical basis of clinical practice*. 39th ed. 287. Elsevier; 2005. pp. 388–389, 403.
9. Mandal L, Mandal SK, Dutta S, Ghosh S, Singh R, Chakraborty SS. Variation of the major sulci of the occipital lobe – a morphological study. *Al Ameen J Med Sci* 2014; 7(2): 141–145.
10. Juch H, Zimine I, Seghier ML, Lazeyras F, Fasel JH. Anatomical variability of the lateral frontal lobe surface: implication for intersubject variability in language neuroimaging. *Neuroimage* 2005; 24(2): 504–514.
11. Tomaiuolo F, MacDonald JD, Caramanos Z, Posner G, Chiavaras M, Evans AC, Petrides M. Morphology, morphometry and probability mapping of the pars opercularis of the inferior frontal gyrus: an in vivo MRI analysis. *Eur J Neurosci* 1999; 11(9): 3033–3046.
12. Ono M, Kubik S, Abernathy CD. *Atlas of the cerebral sulci*. G. Thieme Verlag. New York: Thieme Medical Publishers; 1990.
13. Witelson SF, Kigar DL. Sylvian fissure morphology and asymmetry in men and women: bilateral differences in relation to handedness in men. *J Comp Neurol* 1992; 323(3): 326–340.
14. Boni RC, Prosdócimi FC, Bonsi AB, Almeida TM, Ribeiro LA. Asymmetries of the left and right temporal lobes. *Int J Morphol* 2007; 25(1): 117–120.
15. Retzius G, Andersson S. *Das Menschenhirn: Studien in der makroskopischen Morphologie*. Königlich Buchdruckerei; 1896.
16. Jabeen L, Khalil M, Mannan S, Sultana SZ, Bose SK, Sumi SA, Khan NJ, Nitu NS, Jannat T, Alam MT. A postmortem study of length & depth of the central sulcus in different age & sex groups of Bangladeshi people. *Mymensingh Med J* 2021; 30(2): 368–375.
17. Singh PK, Gupta R. Morphometry of the central sulcus in the brain of Uttar Pradesh region. *Int J Sci Stud* 2015; 3(5): 1–4.

How to cite this article: Nayak S, Gupta C, Hebbar KD, Pandey AK. Morphometric analysis of the main brain sulci and clinical implications: Radiological and cadaveric study. *J Taibah Univ Med Sc* 2023;18(4):676–686.